HHS Public Access

Author manuscript

Circ Res. Author manuscript; available in PMC 2022 October 15.

Published in final edited form as:

Circ Res. 2021 October 15; 129(9): 872–886. doi:10.1161/CIRCRESAHA.121.319828.

PDE1 Inhibition Modulates $Ca_v1.2$ Channel to Stimulate Cardiomyocyte Contraction

Grace K Muller[1], **Joy Song**[1], **Vivek Jani**[1], **Yuejin Wu**[1], **Ting Liu**[1], **William PD Jeffreys**[1], **Brian O'Rourke**[1,3,4], **Mark E Anderson**[1,2,3], **David A Kass**[1,3,4]

[1] Department of Medicine, Division of Cardiology, The Johns Hopkins University School of Medicine, Baltimore, MD, 21205, USA

[2] Department of Physiology, The Johns Hopkins University School of Medicine, Baltimore, MD, 21205, USA

[3] Graduate Program in Cellular and Molecular Medicine, The Johns Hopkins University School of Medicine, Baltimore, MD, 21205, USA

[4] Departments of Pharmacology and Molecular Sciences and Biomedical Engineering, The Johns Hopkins University School of Medicine, Baltimore, MD, 21205, USA

Abstract

Rationale: Cyclic adenosine monophosphate (cAMP) activation of protein kinase A (PKA) stimulates excitation-contraction coupling, increasing cardiac contractility. This is clinically achieved by beta-adrenergic receptor stimulation (b-ARs) or inhibition of phosphodiesterase type-3 (PDE3i), though both approaches are limited by arrhythmia and chronic myocardial toxicity. Phosphodiesterase type-1 inhibition (PDE1i) also augments cAMP and enhances contractility in intact dogs and rabbits. Unlike b-ARs or PDE3i, PDE1i-stimulated inotropy is unaltered by b-AR blockade and induces little whole-cell Ca^{2+} ($[Ca^{2+}]_i$) increase. Positive inotropy from PDE1i was recently reported in human heart failure. However, mechanisms for this effect remain unknown.

Objective: Define the mechanism(s) whereby PDE1i increases myocyte contractility.

Methods and Results: We studied primary guinea pig myocytes that express the PDE1C isoform found in larger mammals and humans. In quiescent cells, the potent, selective PDE1i

Address correspondence to: Dr. David A Kass, Abraham and Virginia Weiss Professor of Cardiology, Department of Medicine, Johns Hopkins University School of Medicine, Baltimore, MD 21205, dkass@jhmi.edu.

DISCLOSURES

DAK is a consultant for Intracellular Therapies, Inc.

SUPPLEMENTAL MATERIAL

Online Figures I–IV

Online Table I: Detailed Statistical Methods and Results for each experiment.

Online Table II: Sample size (number of cells studied and number of guinea pigs from which the cells were obtained) used in each figure panel and assay.

bioRxiv: https://doi.org/10.1101/2020.11.05.368852.

(ITI-214) did not alter cell shortening or $[Ca^{2+}]_i$ whereas b-ARs or PDE3i increased both. When combined with low-dose adenylate cyclase stimulation, PDE1i enhanced shortening in a PKA-dependent manner but unlike PDE3i, induced little $[Ca^{2+}]_i$ rise nor augmented b-ARs. b-ARs or PDE3i reduced myofilament Ca^{2+} sensitivity, and increased SR Ca^{2+} content and phosphorylation of PKA-targeted serines on troponin-I, myosin binding protein C, and phospholamban. PDE1i did not significantly alter any of these. However, PDE1i increased $Ca_v1.2$ channel conductance similarly as PDE3i (both PKA-dependent), without altering NCX current density. Cell shortening and $[Ca^{2+}]_i$ augmented by PDE1i were more sensitive to $Ca_v1.2$ blockade and premature or irregular cell contractions and $[Ca^{2+}]_i$ transients less frequent than with PDE3i.

Conclusions: PDE1i enhances contractility by a PKA-dependent increase in $Ca_v1.2$ conductance with less total $[Ca^{2+}]_i$ increase, and no significant changes in SR $[Ca^{2+}]$, myofilament Ca^{2+}-sensitivity, or phosphorylation of critical EC-coupling proteins as observed with b-ARs and/or PDE3i. PDE1i could provide a novel positive inotropic therapy for heart failure without the toxicities of b-ARs and PDE3i.

Keywords

Basic Science Research; Calcium Cycling/Excitation-Contraction Coupling; Contractile Function; Pharmacology

INTRODUCTION

Heart failure with depressed systolic function is a leading cause of morbidity and mortality that affects tens of millions of patients worldwide[1]. Current therapeutics focus on reducing volume overload with diuretics and blocking β-adrenergic receptor (b-AR) and angiotensin stimulation. Methods to increase contractility have historically mimicked b-AR agonism to increase cyclic adenosine monophosphate (cAMP) that activates protein kinase A (PKA). Although new methods that directly enhance sarcomere function have also been developed[2], current approved methods remain the b-AR agonist dobutamine or phosphodiesterase type-3 (PDE3) inhibitor milrinone that blocks cAMP hydrolysis. The inotropic effects from either are less potent in failing hearts due to downregulation of b-AR signaling and adenylyl cyclase activity[3], and common use of b-AR blockade further curtails their impact in many heart failure patients[4]. Importantly, both approaches also raise intracellular calcium and are pro-arrhythmic, constraining their use to acute indications[5–7]. Safe and effective alternatives remain lacking.

PDE1 is a dual cyclic nucleotide phosphodiesterase highly expressed in the mammalian heart. It is unique among the PDEs because it requires calcium/calmodulin for its activation. There are 3 isoforms, with PDE1C being most prominently expressed in larger mammalian and human hearts, versus PDE1A found in small rodents. This is relevant as PDE1C exhibits balanced selectivity for cAMP and cGMP, whereas PDE1A favors cGMP hydrolysis[8, 9]. In 2018, we first reported that a pan-isoform PDE1 inhibitor (ITI-214) increases contractility and reduces vascular resistance in conscious dogs with normal or failing hearts, and in intact rabbits[8]. These effects were independent of b-AR co-stimulation (b-ARs) or blockade, or to changes in heart rate. Moreover, PDE1 inhibition (PDE1i) regulated cAMP differently than b-ARs or PDE3 inhibition (PDE3i), increasing myocyte contraction with less intracellular

Ca^{2+} concentration ($[Ca^{2+}]_i$) rise. These findings spawned a 2021 Phase Ib-IIa placebo-controlled acute study of ITI-214 in humans with stable heart failure and reduced ejection fraction[10] that found inotropic-vasodilator effects similar to those in dogs and rabbits[8].

The mechanisms by which PDE1i augments contractility, however, remain unknown. PKA activation by b-ARs increases $Ca_v1.2$ (L-type calcium channel) conductance by phosphorylating a regulating peptide – Rad[11, 12]. Concomitantly, PKA phosphorylation of phospholamban (PLN) disinhibits the sarcoplasmic reticulum (SR) Ca^{2+} ATPase (SERCA2a) to increase SR calcium uptake and calcium-induced calcium release[13, 14]. PDE3A localizes to the SR where it regulates cAMP-PKA stimulation[13, 15], and its inhibition further augments SERCA2a activity. Collectively, these changes increase peak calcium transients and quicken their decline, improving contraction and relaxation. At the sarcomere, PKA also phosphorylates troponin I (TnI) to desensitize myofilaments to calcium enhancing relaxation while blunting inotropy, and myosin binding protein C (MYBP-C), accelerating crossbridge kinetics and enhancing b-ARs contraction[16, 17].

Given that calcium transients appear less augmented by PDE1i [8], we speculated that intracellular cAMP-PKA modulation and its downstream consequences differ between PDE1i and b-ARs or PDE3i. The current study tested this hypothesis using guinea pig myocytes that also express the PDE1C isoform as in rabbits and humans. We find that the primary impact of PDE1i is to increase $Ca_v1.2$ conductance without increasing PLN, TnI, or MYBP-C phosphorylation and correspondingly, without altering SR calcium load or myofilament calcium sensitivity. The result is enhanced inotropy with less $[Ca^{2+}]_i$ rise or premature/irregular beats than found with b-ARs and/or PDE3i.

METHODS

Data Availability.

The data that support the findings of this study, are available from the corresponding author upon reasonable request. Except for ITI-214 that was provided directly from Intracellular Therapies Inc. under a research agreement, our study used commercially available reagents that are each identified here and in the Major Resources Table. ITI-214 powder is available for non-human research from MedChemExpress (Cat. No.: HY-12501A).

Reagents.

The following pharmaceuticals were used: ITI-214 (provided under agreement with Intra-Cellular Therapies Inc, NY), cilostamide, forskolin, rolipram (Tocris), caffeine, nitrendipine (Millipore Sigma), Rp-cAMPS and Rp-8-CPT-cAMPS (Cayman Chemical), all but Rp-8-CPT-cAMPS dissolved in 0.1% DMSO (the latter in 0.5% DMSO). The following antibodies were used: PDE1A (Sc-50480, Santa Cruz Biotechnology), PDE1C (Ab14602, Abcam), GAPDH (5174, Cell Signaling), phospho-$Ser^{23/24}$ (4004) and total TnI (4002, both Cell Signaling), phospho-Ser^{273}, -Ser^{282}, -Ser^{302} and total MYBP-C (gifts from Dr. Sakthivel Sadayappan, University of Cincinnati), phospho-Ser^{16} (MA3–922, Badrilla) and total PLN (MA3–922, ThermoFisher Scientific). To obtain single band detection with PDE1C Ab, we used 0.1% KPL (SeraCare) as the blocking buffer. For all other

immunoblots, we used Odyssey Blocking Buffer (Li-Cor) 1:1 in TBST. Please reference the Major Resources Table for further details.

Animals.

Guinea pigs (N=74, males, 350–500 g, ~2–3 month-old) were used in this study. Males were used, as we did not establish any gender-dependent differences upon PDE1 isoform expression pattern. All animal study procedures were performed in accordance with the Guide to the Care and Use of Laboratory Animals and approved by the Johns Hopkins University IACUC.

Myocyte cell isolation.

The protocol used for myocyte isolation is described in detail elsewhere[18]. Briefly, animals were anesthetized with pentobarbital, and hearts rapidly removed via thoracotomy. The aorta was cannulated on a Langendorff apparatus fitted with a heating jacket circulating water at 37°C, and retrograde-perfused for 5 minutes at 8 ml/min with Tyrode's solution. The perfusate was then switched to Tyrode's solution containing collagen type 2 (Worthington) and protease type 14 (Sigma-Aldrich) for 7 minutes. The solution was switched to a modified Kraft-Bruhe (KB) buffer for 5 minutes. The left ventricle was minced and filtered (200μm) to yield single cells. Myocytes rested in KB buffer[19] for an hour before being placed in supplemented M199 ACCIT medium[20].

Sarcomere shortening and Ca^{2+} transients.

Changes in cell sarcomere shortening and Ca^{2+} transients were measured within 7 hours of cell isolation, using a customized IonOptix system[8]. All recordings were performed at 37°C, with pacing stimulation at 1Hz. Cells were loaded using 2μM Fura-2-AM for 15 minutes and then washed for at least 30 minutes. Fura-2 was excited at 340 and 380nm alternating at 250Hz and emission recorded at 510nm by a single PMT. Background was subtracted from Fura-2 readings and the results filtered with a Lowpass Butterworth Filter (cutoff frequency of 10Hz, 2 poles). Ten-15 transients were signal averaged for analysis. The fluorescence ratio value is shown as F/F_0 (fluorescence normalized to baseline 340/360). Baseline recordings were made in Tyrode's with 0.1% DMSO, before stimulation with various agents as described in results. Cells falling within mean ± 2SD for three baseline parameters: pre-stimulation, peak percent change, and time to return to 50% baseline were included for further analysis. To determine the role of PKA in PDE1i or PDE3i mediated response, cells were first pre-incubated with 100μM Rp-8-CPT-cAMPS for 35–45 minutes[21].

To assess SR Ca^{2+} content ($[Ca^{2+}]_{SR}$), caffeine studies were undertaken as described[22]. Caffeine (10mM) was introduced via a needle placed adjacent to the cell. The filtered raw calcium data were fit to single- (systolic transients) or bi- (caffeine transients) exponential decay using a custom MatLab (MathWorks 2018) script. The peak Ca^{2+} transient was determined as the difference in F_{max}-baseline; the decay tau values for the last five paced transients and caffeine-induced release were compared.

Myofilament force-pCa relationship in skinned myocytes.

Myocytes were incubated in 0.3% Triton X-100 in isolation buffer with protease inhibitor (Sigma-Aldrich) and phosphatase inhibitor (PhosSTOP, Roche) for 20 minutes at 10°C as described[23]. After washing in isolation buffer, cells were attached with UV-activated adhesive (Norland Products) to a force transducer-length controller (Aurora Scientific). Sarcomere length was set at 2.1μm by micromanipulators (Siskiyou Corporation) as measured by digital 2D fast Fourier transform of images (IPX-VGA210, Imperx). Tension was equal to force divided by myocyte cross sectional area. Active tension-Ca^{2+} relationships were generated by varying Ca^{2+} concentration from 0 to 46.8 μM. Tension -log[Ca^{2+}] relations were fit to the Hill equation yielding maximal tension (T_{max}), Ca^{2+} sensitivity (EC_{50}), and Hill coefficient[24]. Tension-pCa relationships were normalized to T_{max}.

Cell electrophysiology.

Whole-cell patch clamping was used to measure the Na/Ca exchanger (I_{NCX}) or $Ca_v1.2$ (I_{Ca}) current at 34±1°C, as reported[25, 26]. For NCX: pulses (300ms in duration) were applied from +100 to −100mV in 20mV steps from a holding potential of −40mV. Each cell was recorded under four different conditions as follows: 1) in control bath solution containing 0.1% DMSO, 2) in the presence of indicated drugs without, then 3) with $NiCl_2$ (5mM), and 4) in control solution with $NiCl_2$. Nickel-insensitive currents were subtracted from the corresponding control or drug recordings to derive the nickel-sensitive I_{NCX}. The pipette (intracellular) solution consisted of (in mM): 120 CsCl, 20 HEPES, 5 Mg^{2+}-ATP, 5 1,2-bis(o-aminophenoxy)ethane-N,N,N′,N′-tetraacetic acid (BAPTA), 3 $CaCl_2$ at pH 7.25. The bath (extracellular) solution consisted of (in mM): 130 NaCl, 10 HEPES, 10 glucose, 5 CsCl, 2 $CaCl_2$, 1 MgCl2, pH 7.4, and included 10μM of nitrendipine and thapsigargin to respectively inhibit $Ca_v1.2$ and SERCA.

I_{Ca} was identified by its sensitivity to nitrendipine (10μM). Depolarizing voltage pulses (300ms in duration) to potentials ranging −70 to 60 mV, in 10 mV steps, were applied from a holding potential of −80mV. A pre-pulse to −40mV of 50ms was applied before each step to inactivate Na^+ currents. The pipette solution contained (in mM): 120 CsCl, 10 HEPES, 10 tetraethylammonium (TEA) chloride, 1.0 $MgCl_2$, 1.0 NaGTP, 5.0 phosphocreatine, 3.0 $CaCl_2$, 10 EGTA; pH 7.2 with 1N CsOH. For PKA inhibition, Rp-cAMPS (100μM) was included in the pipette. The bath solution was consisted of (in mM): 137 NaCl, 10 HEPES, 10 glucose, 1.8 $CaCl_2$, 0.5 $MgCl_2$, and 25 CsCl, with pH 7.4 with NaOH.

Western blots.

To probe for PLN phosphorylation, myocytes were incubated with DMSO or various drugs in Tyrode's with 1.8mM Ca^{2+} in a cell suspension for five minutes, rotating at room temperature. Cells were homogenized (Lysis Buffer, Cell Signaling) using beads and mechanical shearing at 30Hz for 2 min (Retsch). The lysates were clarified using centrifugation (2000×g, 10min) and assayed for protein content (BCA Assay, Thermo-Fisher). For sarcomeric proteins, cells were first plated on laminin-coated 6-well plates. The M199 ACCIT media was replaced with identical serum-free media 30 minutes before drug incubation. Cells were treated with DMSO or indicated drugs dissolved in serum-free

media and incubated for 10 minutes at room temperature. Sarcomere fractions were isolated and quantitated as reported[23]. Proteins were separated on gel electrophoresis, followed by hybrid wet transfer onto nitrocellulose. 12% gels were used for PLN; 4–15% gels were used for PDE1A, PDE1C, GAPDH, TnI and MYBP-C. Li-Cor Imager was used to scan and quantitate densitometry values.

Statistical analysis.

Data are plotted along with median and 25/75% in the form of violin plots, or as mean+/−SEM in bar graphs. For analyses with n≥6 per group, normality was tested using D'Agostino-Pearson test. If passed, a parametric analysis, most often 1- or 2-way ANOVA with Šídák's multiple comparisons was used. For all other conditions, non-parametric tests (Kruskal Wallis with Dunn's multiple comparisons test) were used. The specific test type and its results are provided in each figure legend. The Online Table I and II provide further details including complete statistical test output, and number of animals and cells used in each assay. We did not specifically incorporate a group factor for the animal from which myocytes were isolated as an independent covariate in the statistical tests. This is justified for the following reasons. First, all the guinea pigs were healthy and of similar age and sex (male), and the isolation protocol performed was identical for each. Second, the variance in myocyte shortening and calcium transients were similar independent of the number of animals used for any given assay (generally 4 or more). As noted above, only myocytes with baseline characteristics falling within 2SD of the mean were used for analysis which further reduced inter-preparation variance. All exact P values are provided throughout the text, figures, and legends, and statistical results table. $P \leq 0.05$ was considered as statistically significant. All supporting materials and data will be made available upon reasonable request.

RESULTS

Effects of PDE1i on cAMP-stimulated contraction in guinea pig myocytes.

As PDE1 isoform expression had not been previously reported in guinea pig, we first assessed this by Western blot and found both PDE1A and PDE1C are constitutively expressed (Online Figure I) with ratios similar to rabbit and human[8]. Figure 1A–C shows myocyte sarcomere shortening and Ca^{2+} transients in vehicle (0.1% DMSO) and within 5 min exposure to PDE1i ITI-214 (214, 1 μM), PDE3i cilostamide (Cil, 1μM), PDE4i rolipram (Rol, 10μM), or isoproterenol (Iso, 1nM). Both Iso and Cil significantly increased cell shortening and Ca^{2+} transients by amounts that were statistically similar. By contrast, neither Rol nor 214 induced significant changes over baseline. This lack of PDE1i effect on both responses in quiescent guinea pig myocytes is similar to prior findings reported in rabbit myocytes[8]. The lack of PDE4i response is similar to myocyte data from larger mammals that unlike mouse or rat have a more dominant role for PDE3 versus PDE4 on EC coupling[27]. A late Ca^{2+} elevation and sustained shortening as shown in Figure 1A with Cil is fairly common in guinea pig myocytes[28] and due to Na^{+}-Ca^{2+} exchanger (NCX) activity in the reverse mode[29].

As we and others had found inotropic effects from PDE1i require some basal cAMP stimulation [8, 30], we next compared PDE1i or PDE3i effects in cells pre-treated with a low priming dose of the adenylate cyclase stimulator - forskolin (Fsk, 10 or 100 nM, Online Figure IIA). Example sarcomere and Ca^{2+} tracings with 10nM Fsk are displayed in Figure 1D, and group data at both doses in Figures 1E and F. PDE1i significantly increased shortening with borderline trend to increase peak Ca^{2+} transients (P=0.06, P=0.1 with 10nM or 100nM Fsk, respectively). By contrast, PDE3i significantly increased both at either Fsk dose. We chose 1μM 214 based on prior studies[8] and given its nanomolar-range IC_{50}, but also tested if higher doses of ITI-214 (5, 10 μM) in combination with Fsk yielded greater responses. Significant increases in sarcomere shortening were observed at each dose, but they were not statistically different from each other (e.g. no discernable dose response; Online Figure IIB, P=0.37, Kruskal-Wallis with Dunn's post-hoc test). Peak Ca^{2+} significantly increased at 5 or 10 μM, but when compared to each other and 1 μM, the changes were not significantly different (P=0.34). ITI-214 at 10 μM in the absence of Fsk did not significantly change either parameter.

To test whether inotropic enhancement by PDE1i requires PKA activation, we inhibited the kinase using Rp-8-CPT-cAMPS (100μM). This had no significant impact on resting sarcomere shortening but it significantly slowed relaxation rate (Online Figure IIC). In cells then treated with either Fsk+214 or Fsk+Cil, PKA inhibition prevented increased contraction (Figure 1G) and faster relaxation (Online Figure IID). These data support an obligatory role for PKA in the contraction effects from either PDE inhibitor.

Lastly, we tested if PDE1i or PDE3i differentially impact β-AR stimulated sarcomere shortening or Ca^{2+} transients. Both parameters significantly increased with Iso and this was further amplified by co-administration of PDE3i but not PDE1i (Figure 2A, 2B). Taken together, these data reveal distinct responses in myocyte function and Ca^{2+} responses to PDE1i versus PDE3i, yet a similar dependence on PKA activation.

Effects of PDE1i on myofilament tension-Ca^{2+} relations.

Beta-ARs results in phosphorylation of TnI at $Ser^{23/24}$, causing a rightward shift of the myocyte tension-Ca^{2+} dependence (myofilament desensitization) without changing maximal tension[31]. This is parameterized by myofilaments requiring a greater [Ca^{2+}] to generate 50% of the maximal force (EC_{50}). Since PDE1i augmented contraction with little Ca^{2+} change, we speculated it may sensitize or at least not desensitize the myofilaments. We tested this in isolated myocytes incubated with Iso (50nM), Fsk (10nM) + 214 (1μM), or vehicle (DMSO), then chemically skinned and mounted on a force-length apparatus to measure tension-Ca^{2+} relations. Iso significantly shifted this relation rightward, increasing EC_{50} from a mean of 2.4 to 4.6 μM, whereas PDE1i did not shift the relation or alter average EC_{50} (Figure 3A, 3B). Maximal Ca^{2+}-activated tension and cooperativity (Hill coefficient) were not significantly altered with either intervention (Table 1).

The lack of altered tension-Ca^{2+} dependence suggested that PDE1i may not result in PKA phosphorylation of myofilament proteins such as TnI. We tested this by immunoblotting lysates from myocytes exposed to the same stimuli, normalizing results to the maximal response obtained with Fsk+IBMX (100μM). Whereas Iso significantly increased TnI

phosphorylation, Fsk+214 did not (Figure 3C). PKA phosphorylation of MyBP-C also augments contractility following β−ARs[32], and while Iso significantly increased MyBP-C phosphorylation at all three primary PKA-targeted sites Ser[273], Ser[282], and Ser[302], Fsk+214 did not (Figure 3D). Together, these results demonstrate major differences in myofilament modulation and downstream protein phosphorylation comparing PDE1i + Fsk to β-ARs.

Effects of PDE1i on $[Ca^{2+}]_{SR}$ and phospholamban phosphorylation.

The SR is a major intracellular source of Ca^{2+} that b-ARs leverages to increase $[Ca^{2+}]_i$. Here, we tested the effects of PDE1i on $[Ca^{2+}]_{SR}$ and SERCA and its regulator PLN. Myocytes in Fsk (10nM), 214 (1μM), Fsk+214, or Cil (1μM), or vehicle were paced at 0.5 Hz, pacing then stopped, and a caffeine (10μM) bolus applied locally to trigger SR Ca^{2+} release. Fig 4A displays example Ca^{2+} traces for caffeine-induced SR Ca^{2+} release analysis. PDE3i, but not PDE1i (with or without Fsk), increased $[Ca^{2+}]_{SR}$ compare to DMSO vehicle control (Fig 4B).

In paced cells, SERCA2a is primarily responsible for the rapid Ca^{2+} decay rate[33]. We assessed this rate by averaging values from the last five paced transients just prior to caffeine exposure. The rate was significantly increased only with PDE3i (Figure 4C). The decay from peak Ca^{2+} after caffeine-induced release exhibits a bi-exponential course, reflecting contributions of NCX-mediated removal of $[Ca^{2+}]_i$ and then Ca^{2+} buffers as the latter is mostly saturated at initial high $[Ca^{2+}]_i$[33]. We found neither the initial nor subsequent decay rates were significantly changed by any of the stimuli (Fig 4D). To examine NCX current density, we performed patch clamp studies. Neither 214 nor Fsk alone significantly altered the NCX current-voltage dependence as compared to DMSO vehicle (Online Figure III). Though Fsk+214 significantly increased inward current at membrane voltages <−60mV, the reversal potential was also shifted rightward, suggesting activation of another current in this negative voltage range. These data indicate PDE1i does not alter $[Ca^{2+}]_{SR}$ or NCX current density.

PKA-mediated PLN phosphorylation at Ser[16] plays a major role in enhancing SR Ca^{2+} uptake. We therefore examined if Iso and Fsk+214 differ with respect to this post-translational modification. Myocytes exposed to Iso (50nM) showed a consistent, significant rise in Ser[16] phosphorylation that was not observed from Fsk+214 (Fig 4C). This was further explored in cells treated with PDE1i or PDE3i alone, or in combination with non-saturating levels of Iso or Fsk (Figure 4D, 4E). In all conditions, PDE3i significantly elevated PLN phosphorylation over the prior baseline, whereas this was not so with PDE1i. Thus, unlike β-ARs, PDE1i+Fsk does not significantly alter post-translational modification of TnI, MYBP-C, or PLN.

$Ca_v1.2$ channel current increases similarly with PDE1i or PDE3i.

The lack of myofilament or SR modifications by Fsk+PDE1i led us to test its effects upon the primary voltage-sensitive Ca^{2+} channel, $Ca_v1.2$. $Ca_v1.2$ current density was identified by its suppression with nitrendipine as measured by the voltage clamp technique (Fig 5A). Representative current traces are shown for Fsk+214 and Fsk+Cil (Fig 5B). The current-voltage plot was not significantly altered by Fsk or 214 alone compared to vehicle. However,

the combination of the two significantly increased the current density (Fig 5C) by a similar magnitude to that in response to Fsk+Cil. Both were blocked by nitrendipine (10 μM). We further tested if this current rise was PKA dependent by repeating the study after dialyzing cells with Rp-cAMP (100μM). PKA inhibition blocked the effects of PDE1i and PDE3i (Fig 5D).

While Fsk combined with either PDE1i or PDE3i statistically enhanced $Ca_v1.2$ similarly, only the latter condition augmented SR Ca^{2+} release. This suggested Fsk+214 Ca^{2+} transients and shortening would be more sensitive to $Ca_v1.2$ blockade. We tested this by applying nitrendipine over a dose range (Online Figure IV) prior to co-treating cells with either vehicle (DMSO), Fsk+214, or Fsk+Cil. Both Fsk+214 and Fsk+Cil increased shortening (Fig 6A and B) and peak Ca^{2+} transients (Fig 6D and E) that then exhibited a significant dose-dependent decline with nitrendipine. However, the decline was steeper with Fsk+214 by analysis of covariance, supporting greater sensitivity to $Ca_v1.2$ blockade (Fig 6C and D).

Comparison of PDE1i and PDE3i on Ca^{2+}/contraction irregularities.

Increased $[Ca^{2+}]_{SR}$ and/or release is viewed as a potential cause for arrhythmia and is attributed to pro-arrhythmia with both b-ARs and PDE3i. As PDE1i did not significantly alter $[Ca^{2+}]_{SR}$ (unlike PDE3i), we hypothesized cells exposed to this inhibitor with or without Fsk would exhibit less irregularity in Ca^{2+} cycling and corresponding contractions as compared with PDE3i. Myocytes were treated with PDE1i or PDE3i in the presence of 0, 10, or 100 nM Fsk, and examined for rhythm stability (fixed amplitude and rate under paced conditions) or irregularity (both parameters showing variability despite pacing). Figure 7A shows example tracings and Figure 7B summary data for the relative percent of cells with stable versus irregular contractions. PDE3i elicited significantly more irregular contractions and aftercontractions with corresponding changes in Ca^{2+} and shortening, as compared to PDE1i. This was apparent without Fsk (81% vs 5%, $p<0.0001$), and persisted despite Fsk co-stimulation.

DISCUSSION

Selective PDE1i augments cardiac myocyte contractility by distinct mechanisms as compared to PDE3i or β-ARs. Inhibition of PDE1 or PDE3, combined with cAMP synthesis activation, similarly enhances $Ca_v1.2$ current density and increases myocyte contraction. However, PDE1i minimally impacts $[Ca^{2+}]_{SR}$ and correspondingly displays greater negative sensitivity to nitrendipine-induced $Ca_v1.2$ blockade. Furthermore, unlike β-ARs, PDE1i neither augments phosphorylation of TnI at PKA sites nor desensitizes myofilaments to Ca^{2+}. PDE1i also does not increase PLN phosphorylation, consistent with the lack of $[Ca^{2+}]_{SR}$ increase. Lastly, PDE1i triggers fewer irregular Ca^{2+} release and contraction events versus PDE3i. The differences between these stimuli and their downstream effectors are summarized in Figure 8. These findings support a novel method to augment myocyte contraction with potential translational relevance[10].

Evidence for distinct PDE1 vs PDE3 cAMP regulation.

Intrinsic acute increases in cardiac contractility are mostly due to neurohumoral stimulation of cAMP-PKA signaling, and this signaling is in turn countered by the activity of cAMP-targeting PDEs. Each PDE exhibits different compartmentalized signaling and substrate specificity[34]. PDE3 binds cAMP in the nM range[35], whereas PDEs 1 and 4 operate in μM ranges[36]. As intracellular cAMP concentration is ~1 μM[37], PDE3i is expected to readily increase PKA signaling and enhance cell contractility. By contrast, although PDE1i *in vivo* augments contractility, in isolated cells devoid of adrenergic tone, cAMP must first be elevated to observe inotropy as shown here in guinea pig and previously in mouse and rabbit[9, 38].

Spatial compartmentalization of PDEs allows for microdomain regulation of cAMP-PKA signaling[39]. PDE3 is found at the plasma membrane[40] and also at the SR where it controls local Ca^{2+} uptake[15]. PDE1 also displays immunofluorescence staining along Z- and M-lines in human myocytes[41]. However, PDE1 accounts for only 14% of microsomal PDE activity against cAMP as compared to 78% in the cytoplasmic fraction. This contrasts with PDE3, which contributes 69% of cAMP esterase activity in microsomal fractions of myocytes from large mammalian hearts which includes the SR[41]. These spatial differences may well explain why PDE1i does not phosphorylate PLN or modulate $[Ca^{2+}]_{SR}$.

PDE3i or PDE1i increased $Ca_v1.2$ current similarly, placing both PDEs within caveolin-enriched microdomains of the sarcolemma,[42, 43] where this channel resides[44]. The requirement of PDE1 activity on Ca^{2+}-calmodulin that is itself triggered by $Ca_v1.2$ activation raises the intriguing possibility that PDE1 is a negative regulator of $Ca_v1.2$ current by reducing its stimulation by cAMP-PKA. However, unlike PDE1i, PDE3i amplifies Ca^{2+} and shortening stimulated by Iso, revealing substantial differences in their interaction with β-AR agonism. This suggests that while proximate to the channel, the two PDEs likely reside in different nanodomains. Beta-adrenergic stimulated $Ca_v1.2$ current requires Rad phosphorylation to relieve its constitutive suppression of I_{Ca}[11, 12]. Proximity protein analysis identified several PDE4 isoforms, PDE3A, and PDE1C as all being near $Ca_v1.2$ [11]. PDE1C is also found in a complex with adenosine A_2 receptors and the non-selective cation channel transient receptor potential cation channel 3 (TRPC3), where it plays a role in cytoprotective signaling[45]. This is intriguing as TRPC3 conductance is also nickel insensitive, and so could be the source of increased inward non-NCX current we observed with Fsk-214.

PDE1i control of myocyte contraction.

These new findings have clinical relevance as ITI-214 was recently tested in humans with heart failure in a study that revealed inotropic and vasodilator effects with negligible rhythm disturbance[10]. Our prior study in rabbits found PDE1i induces less Ca^{2+} rise than PDE3i or β-ARs[8], findings we confirm here in the guinea pig. The new data further now reveal PDE1i modulation is PKA dependent and targets $Ca_v1.2$ without altering SERCA2a or NCX function. Inotropy was accompanied by a slight rise in peak $[Ca^{2+}]_i$ that did not reach statistical significance. While any rise in $[Ca^{2+}]_i$ would be expected to increase SR stores, the level appears too low to be detected with the whole cell detection assay we used, and is at least significantly lower than induced by PDE3i. Even without significant

SR Ca^{2+} release, the rise in $Ca_v1.2$-mediated Ca^{2+} entry can be sufficient to stimulate contraction. PDE1i did not concomitantly lower myofilament Ca^{2+} sensitivity, a finding further supported by its lack of TnI phosphorylation. As Ca^{2+} desensitization is normally observed with Iso, this means with PDE1i, increased myofibrillar force can be achieved at a lower $[Ca^{2+}]_i$. In addition, $Ca_v1.2$ accounts for ~30% of the total Ca^{2+} rise in guinea pig myocytes[46], similar to levels found in larger mammals and humans. This means a given change in $Ca_v1.2$ current can be more influential than might be in rat or mouse, in which the SR dominates and sarcolemmal Ca^{2+} influx contributes <10% to the total transient. While NCX current density was unaltered, the exchanger would still be expected to transport an increase in intracellular Ca^{2+} in the forward mode to restore the net balance. There are other potential mediators including mitochondrial Ca^{2+} uptake, the sarcolemmal Ca^{2+} ATPase, and intracellular Ca^{2+} buffers, though these handle smaller amounts of Ca^{2+}. Together our data support a PDE1i mediated increase in sarcolemmal Ca^{2+} cycling.

PDE3i induced premature and irregular Ca^{2+} release and associated extra contractions in myocytes, consistent with its known pro-arrhythmic effects. While some irregularity was also observed with PDE1i, this was less frequent. To date, studies with ITI-214 in humans with Parkinson's disease or dilated cardiomyopathy have not found pro-arrhythmic effects[10, 47], nor does the compound trigger arrhythmia in intact dogs (± heart failure) or in rabbits[8]. This contrasts to heart failure studies using PDE3i, which trigger increased arrhythmias even upon acute exposure[48, 49]. Whether this applies to chronic treatment with a PDE1i remains to be tested.

Limitations.

Our study leaves several questions unanswered. The precise localization of the PDE1-regulated cAMP microdomains, and identity of the proteins directly impacted by its inhibition remain unknown. Active studies employing locally targeted fluorescent resonance energy transfer probes and proximity labeling and phospho-proteomics hope to address this knowledge gap. As mentioned, it remains possible that some modest SR Ca^{2+} uptake occurs but was not detected in our measurement of change in $[Ca^{2+}]_i$ with Fura-2. Measurement of $[Ca^{2+}]_{SR}$ release using an intra-SR sensor or one targeted to the SR membrane might reveal low amplitude changes. Lastly, while the contraction/Ca^{2+} responses were PKA dependent and so indicate cAMP is the primary regulated species, a potential role for cGMP remains. PDE1A, which preferentially hydrolyzes cGMP >20x more than cAMP, is also expressed in larger mammals and humans. ITI-214 is not PDE1 isoform selective[50] since the catalytic site is highly homologous among the isoforms. However, cGMP elevation has not been demonstrated to augment $Ca_v1.2$, with one study reporting the opposite effect[51].

Conclusions.

PDE1i increases $Ca_v1.2$ activity in a PKA-dependent manner, increasing myocyte contraction in cells pre-stimulated with adenylyl cyclase activator. Unlike PDE3i, PDE1i modulation occurs independent of b-ARs. Moreover, PDE1i neither phosphorylates PLN, TnI, or MYBP-C, nor alters $[Ca^{2+}]_{SR}$ load or myofilament Ca^{2+} sensitivity. The data support a regulatory role of PDE1 on $Ca_v1.2$, with inotropic effects likely augmented by a lack of concomitant myofilament Ca^{2+} desensitization. The integrated result is cAMP/

PKA-dependent inotropy with less Ca^{2+} and less rhythm disturbance. Future studies should clarify the use of PDE1i as a heart disease therapy.

Supplementary Material

Refer to Web version on PubMed Central for supplementary material.

ACKNOWLEDGEMENTS

We thank Dr. Sakthivel Sadayappan for myosin binding protein-C antibodies; Drs. Kobra Haghighi and Litsa Kranias for technical advice on phospholamban westerns; and Ms. Laurel Keefer for her assistance in R coding language. ITI-214 was provided by Intracellular Therapies Inc. under a research agreement with JHU.

SOURCES OF FUNDING

This work was supported by AHA 18POST33960157 and 20CDA35260135 (GKM), R35 HL140034 (MEA), NIH R01HL134821 (BOR), and AHA 16SFRN28620000, NIH R35 HL135827, RO1 HL-114910, and research support from Intracellular Therapies Inc. (DAK).

Nonstandard Abbreviations and Acronyms:

b-ARs	b adrenergic receptor stimulation
PDE1i	phosphodiesterase type-1 inhibition
PDE3i	phosphodiesterase type-3 inhibition
PLN	phospholamban
SR	sarcoplasmic reticulum
TnI	troponin I
MYBP-C	myosin binding protein C

REFERENCES

1. Conrad N, Judge A, Tran J, Mohseni H, Hedgecott D, Crespillo AP, Allison M, Hemingway H, Cleland JG, McMurray JJV, Rahimi K. Temporal trends and patterns in heart failure incidence: A population-based study of 4 million individuals. Lancet. 2018;391:572–580 [PubMed: 29174292]
2. Teerlink JR, Diaz R, Felker GM, McMurray JJV, Metra M, Solomon SD, Adams KF, Anand I, Arias-Mendoza A, Biering-Sørensen T, Böhm M, Bonderman D, Cleland JGF, Corbalan R, Crespo-Leiro MG, Dahlström U, Echeverria LE, Fang JC, Filippatos G, Fonseca C, Goncalvesova E, Goudev AR, Howlett JG, Lanfear DE, Li J, Lund M, Macdonald P, Mareev V, Momomura SI, O'Meara E, Parkhomenko A, Ponikowski P, Ramires FJA, Serpytis P, Sliwa K, Spinar J, Suter TM, Tomcsanyi J, Vandekerckhove H, Vinereanu D, Voors AA, Yilmaz MB, Zannad F, Sharpsten L, Legg JC, Varin C, Honarpour N, Abbasi SA, Malik FI, Kurtz CE. Cardiac myosin activation with omecamtiv mecarbil in systolic heart failure. N Engl J Med. 2021;384:105–116 [PubMed: 33185990]
3. Movsesian MA, Bristow MR. Alterations in camp-mediated signaling and their role in the pathophysiology of dilated cardiomyopathy. Curr.Top.Dev.Biol 2005;68:25–48 [PubMed: 16124995]
4. Bistola V, Arfaras-Melainis A, Polyzogopoulou E, Ikonomidis I, Parissis J. Inotropes in acute heart failure: From guidelines to practical use: Therapeutic options and clinical practice. Card Fail Rev. 2019;5:133–139 [PubMed: 31768269]

5. Felker GM, Benza RL, Chandler AB, Leimberger JD, Cuffe MS, Califf RM, Gheorghiade M, O'Connor CM, Investigators O-C. Heart failure etiology and response to milrinone in decompensated heart failure: Results from the optime-chf study. J Am Coll Cardiol. 2003;41:997–1003 [PubMed: 12651048]
6. Abraham W, Adams K, Fonarow G, Costanzo M, Berkowitz R, LeJemtel T, Cheng M, Wynne J, Investigators ASACa, Group AS. In-hospital mortality in patients with acute decompensated heart failure requiring intravenous vasoactive medications: An analysis from the acute decompensated heart failure national registry (adhere). Journal of the American College of Cardiology. 2005;46:57–64 [PubMed: 15992636]
7. Packer M, Carver JR, Rodeheffer RJ, Ivanhoe RJ, DiBianco R, Zeldis SM, Hendrix GH, Bommer WJ, Elkayam U, Kukin ML, et al. Effect of oral milrinone on mortality in severe chronic heart failure. The promise study research group. N Engl J Med. 1991;325:1468–1475 [PubMed: 1944425]
8. Hashimoto T, Kim GE, Tunin RS, Adesiyun T, Hsu S, Nakagawa R, Zhu G, O'Brien JJ, Hendrick JP, Davis RE, Yao W, Beard D, Hoxie HR, Wennogle LP, Lee DI, Kass DA. Acute enhancement of cardiac function by phosphodiesterase type 1 inhibition. Circulation. 2018;138:1974–1987 [PubMed: 30030415]
9. Bender AT, Beavo JA. Cyclic nucleotide phosphodiesterases: Molecular regulation to clinical use. Pharmacol Rev. 2006;58:488–520 [PubMed: 16968949]
10. Gilotra NA, DeVore AD, Povsic TJ, Hays AG, Hahn VS, Agunbiade TA, DeLong A, Satlin A, Chen R, Davis R, Kass DA. Acute hemodynamic effects and tolerability of phosphodiesterase 1-inhibition with iti-214 in human systolic heart failure Circ Heart Fail. 2021;In Press (DOI: 10.1161/CIRCHEARTFAILURE.120.008236.
11. Liu G, Papa A, Katchman A, Zakharov S, Roybal D, Hennessey J, Kushner J, Yang L, Chen B, Kushnir A, Dangas K, Gygi S, Pitt G, Colecraft H, Ben-Johny M, Kalocsay M, Marx S. Mechanism of adrenergic ca v 1.2 stimulation revealed by proximity proteomics. Nature. 2020;577:695–700 [PubMed: 31969708]
12. Papa A, Kushner JS, Hennessey JA, Katchman AN, Zakharov SI, Chen B-X, Yang L, Lu R, Leong S, Diaz J, Liu G, Roybal DD, Liao X, del Rivero Morfin P, Colecraft HM, Pitt GS, Clarke OB, V.K. T, Johny MB, Marx SO. Adrenergic $ca_v1.2$ activation via rad phosphorylation converges at $alpha_{1c}$ i-ii loop. Circulation Research. 2020;0
13. Beca S, Ahmad F, Shen W, Liu J, Makary S, Polidovitch N, Sun J, Hockman S, Chung YW, Movsesian M, Murphy E, Manganiello V, Backx PH. Phosphodiesterase type 3a regulates basal myocardial contractility through interacting with sarcoplasmic reticulum calcium atpase type 2a signaling complexes in mouse heart. Circ Res. 2013;112:289–297 [PubMed: 23168336]
14. Haghighi K, Kolokathis F, Gramolini AO, Waggoner JR, Pater L, Lynch RA, Fan GC, Tsiapras D, Parekh RR, Dorn GW 2nd, MacLennan DH, Kremastinos DT, Kranias EG. A mutation in the human phospholamban gene, deleting arginine 14, results in lethal, hereditary cardiomyopathy. Proc Natl Acad Sci U S A. 2006;103:1388–1393 [PubMed: 16432188]
15. Ahmad F, Shen W, Vandeput F, Szabo-Fresnais N, Krall J, Degerman E, Goetz F, Klussmann E, Movsesian M, Manganiello V. Regulation of sarcoplasmic reticulum ca2+ atpase 2 (serca2) activity by phosphodiesterase 3a (pde3a) in human myocardium: Phosphorylation-dependent interaction of pde3a1 with serca2. J Biol Chem. 2015;290:6763–6776 [PubMed: 25593322]
16. Moss RL, Fitzsimons DP, Ralphe JC. Cardiac mybp-c regulates the rate and force of contraction in mammalian myocardium. Circ Res. 2015;116:183–192 [PubMed: 25552695]
17. Streng AS, de Boer D, van der Velden J, van Dieijen-Visser MP, Wodzig WK. Posttranslational modifications of cardiac troponin t: An overview. J Mol Cell Cardiol. 2013;63:47–56 [PubMed: 23871791]
18. Liu T, Takimoto E, Dimaano VL, DeMazumder D, Kettlewell S, Smith G, Sidor A, Abraham TP, O'Rourke B. Inhibiting mitochondrial na+/ca2+ exchange prevents sudden death in a guinea pig model of heart failure. Circ Res. 2014;115:44–54 [PubMed: 24780171]
19. Isenberg G, Klockner U. Calcium tolerant ventricular myocytes prepared by preincubation in a "Kb medium". Pflugers Arch. 1982;395:6–18 [PubMed: 7177773]
20. Ellingsen O, Davidoff AJ, Prasad SK, Berger HJ, Springhorn JP, Marsh JD, Kelly RA, Smith TW. Adult rat ventricular myocytes cultured in defined medium: Phenotype and electromechanical function. Am J Physiol. 1993;265:H747–754 [PubMed: 8368376]

21. Money-Kyrle AR, Davies CH, Ranu HK, O'Gara P, Kent NS, Poole-Wilson PA, Harding SE. The role of camp in the frequency-dependent changes in contraction of guinea-pig cardiomyocytes. Cardiovasc Res. 1998;37:532–540 [PubMed: 9614507]
22. Tang M, Zhang X, Li Y, Guan Y, Ai X, Szeto C, Nakayama H, Zhang H, Ge S, Molkentin JD, Houser SR, Chen X. Enhanced basal contractility but reduced excitation-contraction coupling efficiency and beta-adrenergic reserve of hearts with increased cav1.2 activity. Am J Physiol Heart Circ Physiol. 2010;299:H519–528 [PubMed: 20543081]
23. Kirk JA, Holewinski RJ, Kooij V, Agnetti G, Tunin RS, Witayavanitkul N, de Tombe PP, Gao WD, Van Eyk J, Kass DA. Cardiac resynchronization sensitizes the sarcomere to calcium by reactivating gsk-3beta. J Clin Invest. 2014;124:129–138 [PubMed: 24292707]
24. Hsu S, Kokkonen-Simon KM, Kirk JA, Kolb TM, Damico RL, Mathai SC, Mukherjee M, Shah AA, Wigley FM, Margulies KB, Hassoun PM, Halushka MK, Tedford RJ, Kass DA. Right ventricular myofilament functional differences in humans with systemic sclerosis-associated versus idiopathic pulmonary arterial hypertension. Circulation. 2018;137:2360–2370 [PubMed: 29352073]
25. Rasmussen T, Wu Y, Joiner M, Koval O, Wilson N, Luczak E, Wang Q, Chen B, Gao Z, Zhu Z, Wagner B, Soto J, McCormick M, Kutschke W, Weiss R, Yu L, Boudreau R, Abel E, Zhan F, Spitz D, Buettner G, Song L, Zingman L, Anderson M. Inhibition of mcu forces extramitochondrial adaptations governing physiological and pathological stress responses in heart. Proceedings of the National Academy of Sciences of the United States of America. 2015;112:9129–9134 [PubMed: 26153425]
26. Liu T, O'Rourke B. Regulation of the na+/ca2+ exchanger by pyridine nucleotide redox potential in ventricular myocytes. J Biol Chem. 2013;288:31984–31992 [PubMed: 24045952]
27. Richter W, Xie M, Scheitrum C, Krall J, Movsesian M, Conti M. Conserved expression and functions of pde4 in rodent and human heart. Basic research in cardiology. 2011;106:249–262 [PubMed: 21161247]
28. Liu T, Yang N, Sidor A, O'Rourke B. Mcu overexpression rescues inotropy and reverses heart failure by reducing sr ca 2+ leak. Circulation research. 2021;128:1191–1204 [PubMed: 33522833]
29. Grantham CJ, Cannell MB. Ca2+ influx during the cardiac action potential in guinea pig ventricular myocytes. Circulation Research. 1996:194–200 [PubMed: 8755995]
30. Sprenger JU, Bork NI, Herting J, Fischer TH, Nikolaev VO. Interactions of calcium fluctuations during cardiomyocyte contraction with real-time camp dynamics detected by fret. PloS one. 2016;11:e0167974 [PubMed: 27930744]
31. Gambassi G, Spurgeon H, Lakatta E, Blank P, Capogrossi M. Different effects of alpha- and beta-adrenergic stimulation on cytosolic ph and myofilament responsiveness to ca2+ in cardiac myocytes. Circulation research. 1992;71:870–882 [PubMed: 1516160]
32. Mohamed AS, Dignam JD, Schlender KK. Cardiac myosin-binding protein c (mybp-c): Identification of protein kinase a and protein kinase c phosphorylation sites. Arch Biochem Biophys. 1998;358:313–319 [PubMed: 9784245]
33. Díaz ME, Trafford AW, Eisner DA. The role of intracellular ca buffers in determining the shape of the systolic ca transient in cardiac ventricular myocytes. Pflugers Archiv : European journal of physiology. 2001;442:96–100 [PubMed: 11374074]
34. Kokkonen K, Kass DA. Nanodomain regulation of cardiac cyclic nucleotide signaling by phosphodiesterases. Annual review of pharmacology and toxicology. 2017;57:455–479
35. Manganiello V, Murata T, Taira M, Belfrage P, Degerman E. Diversity in cyclic nucleotide phosphodiesterase isoenzyme families. Archives of biochemistry and biophysics. 1995;322:1–13 [PubMed: 7574662]
36. Kim GE, Kass DA. Cardiac phosphodiesterases and their modulation for treating heart disease. In: Bauersachs J, Butler J, Sandner P, eds. Heart failure. Springer, Cham; 2017:249–269.
37. Koschinski A, Zaccolo M. Quantification and comparison of signals generated by different fret-based camp reporters. Methods Mol Biol. 2019;1947:217–237 [PubMed: 30969419]
38. Salanova M, Jin S, Conti M. Heterologous expression and purification of recombinant rolipram-sensitive cyclic amp-specific phosphodiesterases. Methods (San Diego, Calif.). 1998;14:55–64

39. Surdo NC, Berrera M, Koschinski A, Brescia M, Machado MR, Carr C, Wright P, Gorelik J, Morotti S, Grandi E, Bers DM, Pantano S, Zaccolo M. Fret biosensor uncovers camp nano-domains at β-adrenergic targets that dictate precise tuning of cardiac contractility. Nature Communications. 2017;8:15031
40. Sun B, Li H, Shakur Y, Hensley J, Hockman S, Kambayashi J, Manganiello VC, Liu Y. Role of phosphodiesterase type 3a and 3b in regulating platelet and cardiac function using subtype-selective knockout mice. Cell Signal. 2007;19:1765–1771 [PubMed: 17482796]
41. Vandeput F, Wolda SL, Krall J, Hambleton R, Uher L, McCaw KN, Radwanski PB, Florio V, Movsesian MA. Cyclic nucleotide phosphodiesterase pde1c1 in human cardiac myocytes. J Biol Chem. 2007;282:32749–32757 [PubMed: 17726023]
42. Kawai M, Hussain M, Orchard C. Excitation-contraction coupling in rat ventricular myocytes after formamide-induced detubulation. The American journal of physiology. 1999;277:H603–609 [PubMed: 10444485]
43. Pásek M, Brette F, Nelson A, Pearce C, Qaiser A, Christe G, Orchard C. Quantification of t-tubule area and protein distribution in rat cardiac ventricular myocytes. Progress in biophysics and molecular biology. 2008;96:244–257 [PubMed: 17881039]
44. Bhargava A, Lin X, Novak P, Mehta K, Korchev Y, Delmar M, Gorelik J. Super-resolution scanning patch clamp reveals clustering of functional ion channels in adult ventricular myocyte. Circ Res. 2013;112:1112–1120 [PubMed: 23438901]
45. Zhang Y, Knight W, Chen S, Mohan A, Yan C. A multi-protein complex with trpc, pde1c, and a2r plays a critical role in regulating cardiomyocyte camp and survival. Circulation. 2018
46. Bers DM. Calcium cycling and signaling in cardiac myocytes. Annu Rev Physiol. 2008;70:23–49 [PubMed: 17988210]
47. Davis R, Riesenberg R, Laskowitz D, Guptill J, Sanders L, Cooney J, Satlin A, O'Brien J, Duthiel S, Cruz S, Hendrick J, Li P, Wennogle L, Glass S, Pinho M, Taylor E, Kozauer S, Weingart M, Mates S, Snyder G, Vanover K. Iti-214, a novel phosphodiesterase i inhibitor for the treatment of parkinson's disease: Results from a phase i/ii clinical study (p2.8–051). Neurology. 2019;92:P2.8–051
48. Kittleson M, Johnson L, Pion P. The acute hemodynamic effects of milrinone in dogs with severe idiopathic myocardial failure. Journal of veterinary internal medicine. 1987;1:121–127 [PubMed: 3506096]
49. Anderson J, Askins J, Gilbert E, Menlove R, Lutz J. Occurrence of ventricular arrhythmias in patients receiving acute and chronic infusions of milrinone. American heart journal. 1986;111:466–474 [PubMed: 3953354]
50. Snyder GL, Prickaerts J, Wadenberg ML, Zhang L, Zheng H, Yao W, Akkerman S, Zhu H, Hendrick JP, Vanover KE, Davis R, Li P, Mates S, Wennogle LP. Preclinical profile of iti-214, an inhibitor of phosphodiesterase 1, for enhancement of memory performance in rats. Psychopharmacology (Berl). 2016;233:3113–3124 [PubMed: 27342643]
51. Yang L, Liu G, Zakharov SI, Bellinger AM, Mongillo M, Marx SO. Protein kinase g phosphorylates cav1.2 alpha1c and beta2 subunits. Circ Res. 2007;101:465–474 [PubMed: 17626895]

NOVELTY AND SIGNIFICANCE

What Is Known?

- Stimulation of beta-1 adrenergic receptors (b1-AR) or inhibition of phosphodiesterase type 3 (PDE3) augments cAMP to activate protein kinase A (PKA), and both approaches are clinically used to acutely enhance ventricular contractility in patients with heart failure.
- However, each approach also increases myocyte calcium to achieve their effects, and this is associated with a pro-arrhythmic effect that has limited their use.
- In large mammals including humans, inhibiting the dual cyclic-nucleotide regulating phosphodiesterase PDE1 augments ventricular contractility, and in experimental studies, this occurs with a rise in cyclic AMP but less whole cell calcium increase than from b1-AR stimulation or PDE3 inhibition.

What New Information Does This Article Contribute?

- PDE1 inhibition augments myocyte contractility in a PKA dependent manner by increasing CaV1.2 channel activity but unlike PDE3 inhibition, does not alter sarcoplasmic reticular calcium storage or cycling.
- Unlike b1-AR, PDE1 inhibition does not increase phosphorylation of phospholamban, troponin I, or myosin binding protein C at PKA targeted sites and does not reduce myofilament calcium sensitivity to calcium.
- Myocytes exhibit far less irregular calcium cycling and associated arrhythmia in response to PDE1 inhibition as compared to PDE3 inhibition.

We previously reported that PDE1 inhibition augments ventricular contractility in intact dogs and rabbits but with less rise in myocyte whole cell calcium as compared to b1-AR stimulation or PDE3 inhibition. PDE1 inhibition did not amplify cardiac or myocyte inotropy from b1-AR, unlike PDE3 inhibition. However, the mechanism for inotropy by PDE1 inhibition remained unknown. Here, we show PDE1 inhibition induces a PKA-dependent increase in calcium conductance via the L-type calcium channel (CaV1.2) but has negligible impact on calcium uptake and storage into the sarcoplasmic reticulum (SR), unlike PDE3 inhibition that increases both. Phospholamban phosphorylation increases with isoproterenol and PDE3 inhibition but not PDE1 inhibition. Moreover, whereas b1-AR desensitizes myofilaments to calcium associated with PKA phosphorylation of troponin I, this also does not occur with PDE1 inhibition. This means that contractility can be increased with less intracellular myocyte calcium rise. Lastly, myocytes display less irregular calcium release and associated arrhythmia to PDE1 versus PDE3 inhibition. ITI-214, the PDE1 inhibitor employed in this study was recently tested in humans with Parkinson’s disease and stable heart failure, the latter finding positive inotropy with no significant heart rhythm change. Further chronic studies in heart failure patients are warranted.

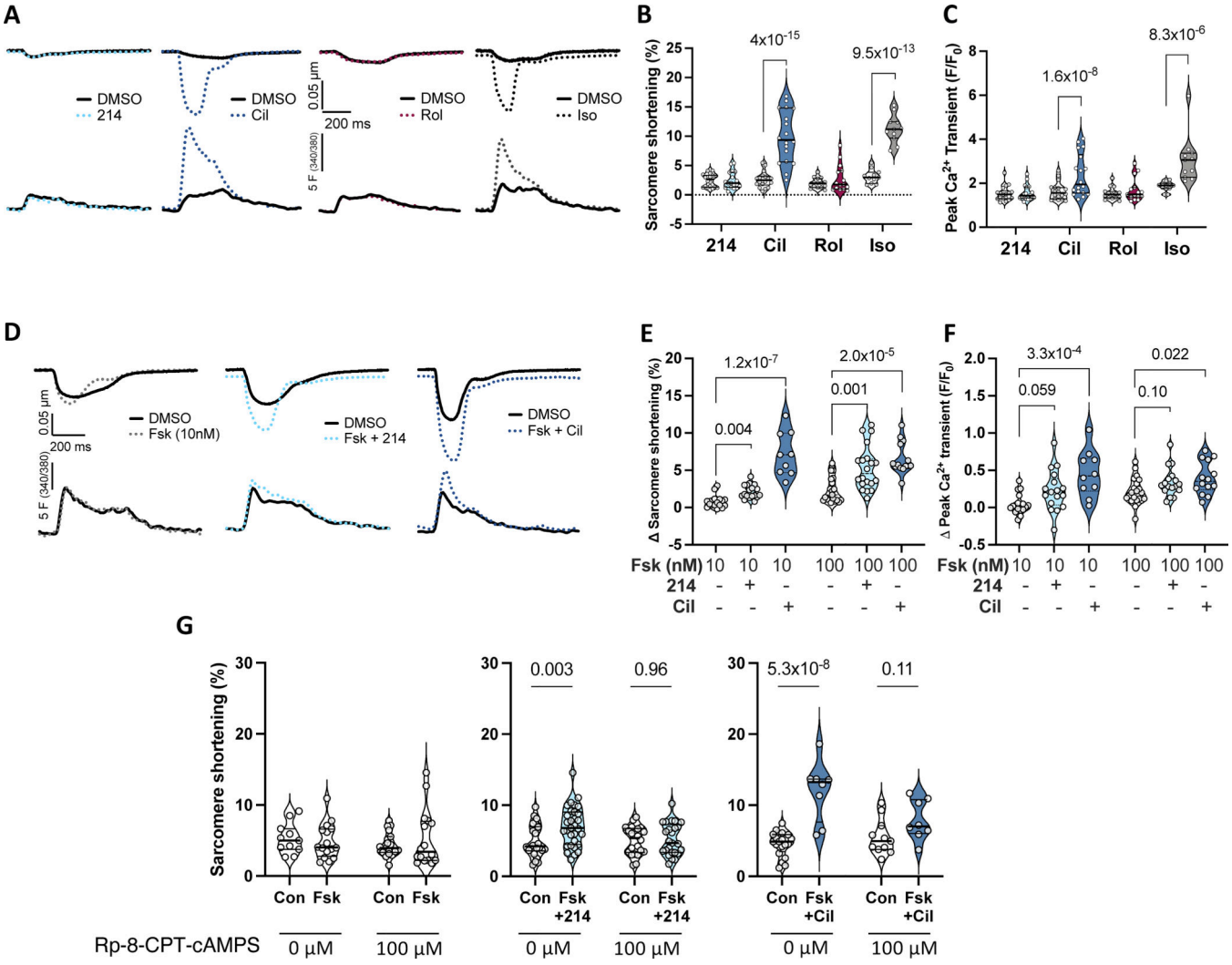

Figure 1. PDE1i stimulates contraction at less Ca^{2+} rise than PDE3i in guinea pig.

A) Representative sarcomere shortening (upper) and Ca^{2+} transients (lower) from cardiomyocytes treated with a selective inhibitor to PDE1 (214; 1μM), PDE3 (cilostamide - Cil; 1μM), PDE4 (rolipram - Rol; 10μM), or isoproterenol (Iso; 1nM) each in 0.1% DMSO versus DMSO alone. **B, C)** Summary data pairing before and after drug (clear and shaded background, respectively); repeated measures 2-way ANOVA and Sidak's multiple comparison test (MCT) within each drug (P values shown). **D)** Impact of PDE1 vs PDE3 inhibition in presence of 10nM Fsk versus Fsk alone. **E, F)** Group data showing change from baseline for this experiment using either 10 or 100 nM Fsk; Kruskal-Wallis test within each Fsk dose; Dunn's MCT P-values shown. **G)** Change in sarcomere shortening in absence or presence of PKA inhibitor (Rp-8-CPT-cAMPS, 100μM) in same treatment groups shown in panels **D-F**. Ordinary 2-way ANOVA with Sidak's MCT for effect of PDE inhibitor ±PKA inhibitor. Interaction of PDEi and PKA inhibitor effects were P=0.047 and P=0.0035 for Fsk+214 and Fsk+Cil, respectively.

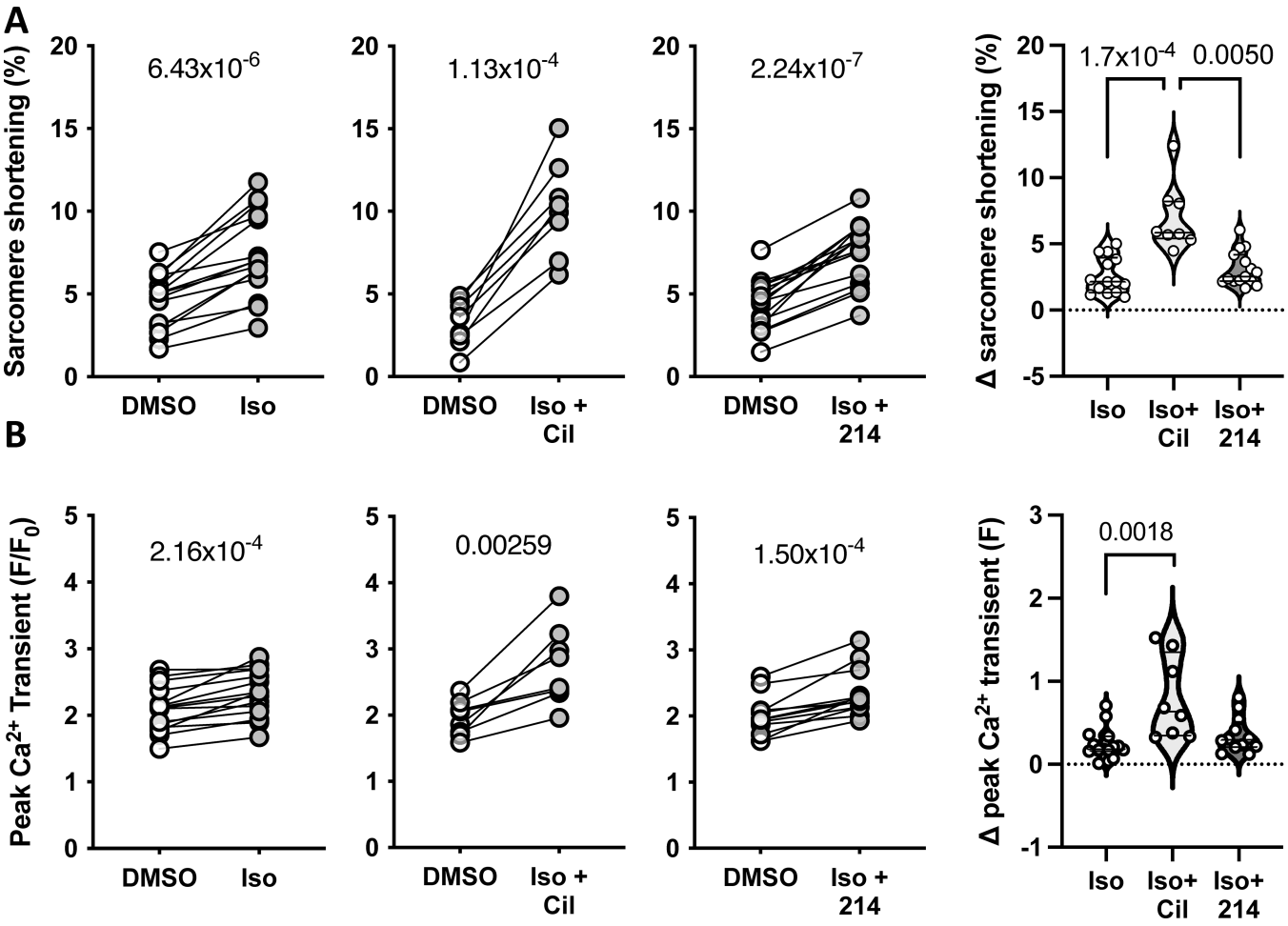

Figure 2. PDE1-i vs PDE3-i modulation of β-AR-stimulated signaling.

Guinea pig myocytes were treated with sub-maximal isoproterenol (Iso; 0.025nM) alone, or with Cil or 214. Changes in the peak **A)** sarcomere shortening and **B)** Ca^{2+} transients are plotted, with p-values indicating paired Student's t-test results. The change from baseline is plotted to the right; P values are for a Kruskal-Wallis test with Dunn's MCT.

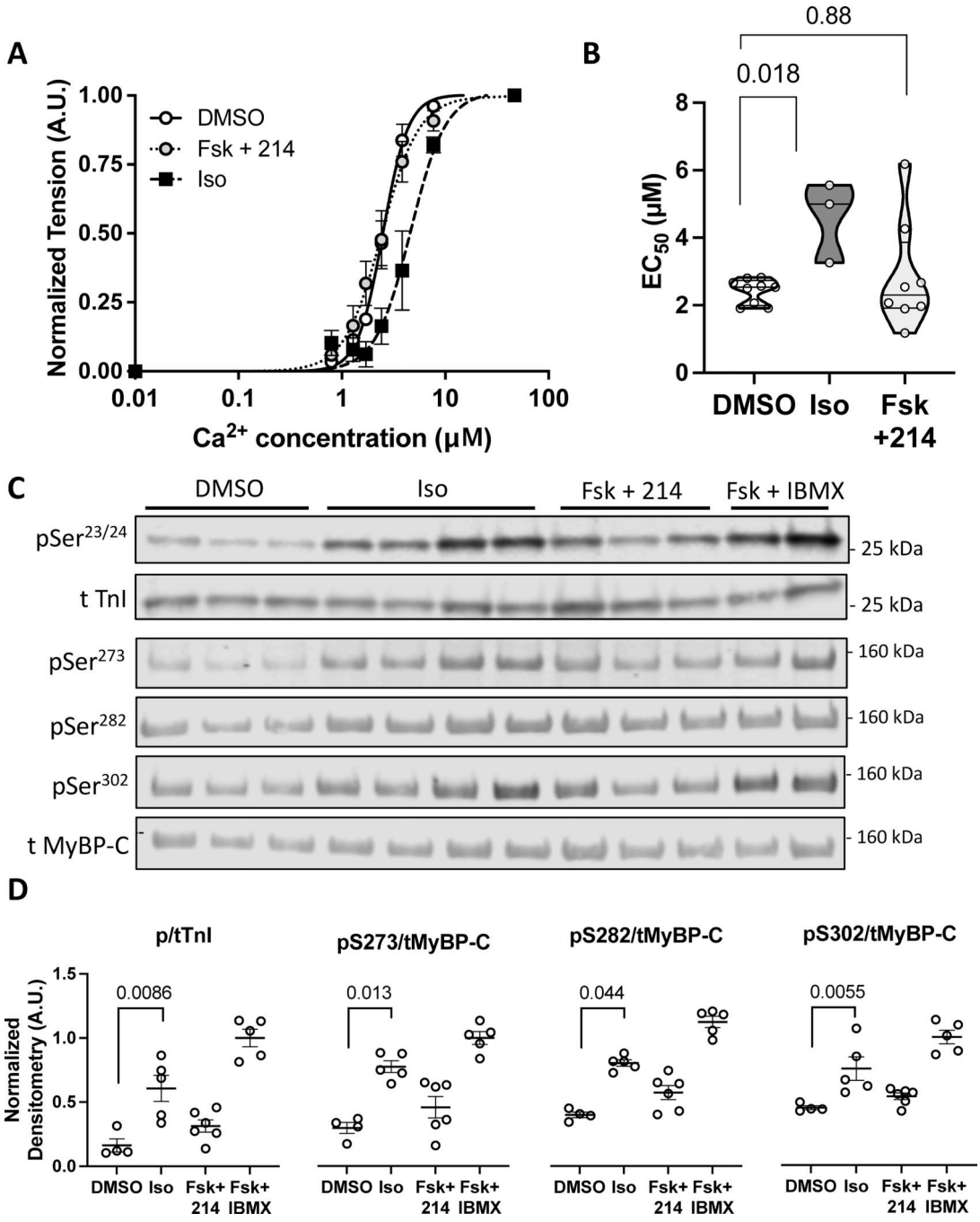

Figure 3. Effects of PDE1i upon myofilament-Ca relationship and PKA-mediated phosphorylation of TnI or MYBP-C.

Guinea pig myocytes were treated with DMSO, Iso (50nM), or Fsk (10nM) + 214 (1μM) before being skinned. **A)** A normalized curve showing the myofilament force-pCa relationship; n=9, 9, 3. **B)** Summary EC_{50} (Ca^{2+} at 50% maximal activation) for each condition. P-values are Mann-Whitney U test with 2-comparison correction. **C)** Representative western blot of phosphorylated and total troponin I (TnI) at $Ser^{23/24}$ or myosin binding protein-C (MyBP-C) at Ser^{273}, Ser^{282} and Ser^{302} for myocytes treated as

indicated. **D)** The phospho/total densitometry values as indicated were normalized to a maximal response from Fsk (25μM) + IBMX (100μM). Kruskal-Wallis test with Dunn's MCT among DMSO, Iso and Fsk+214.

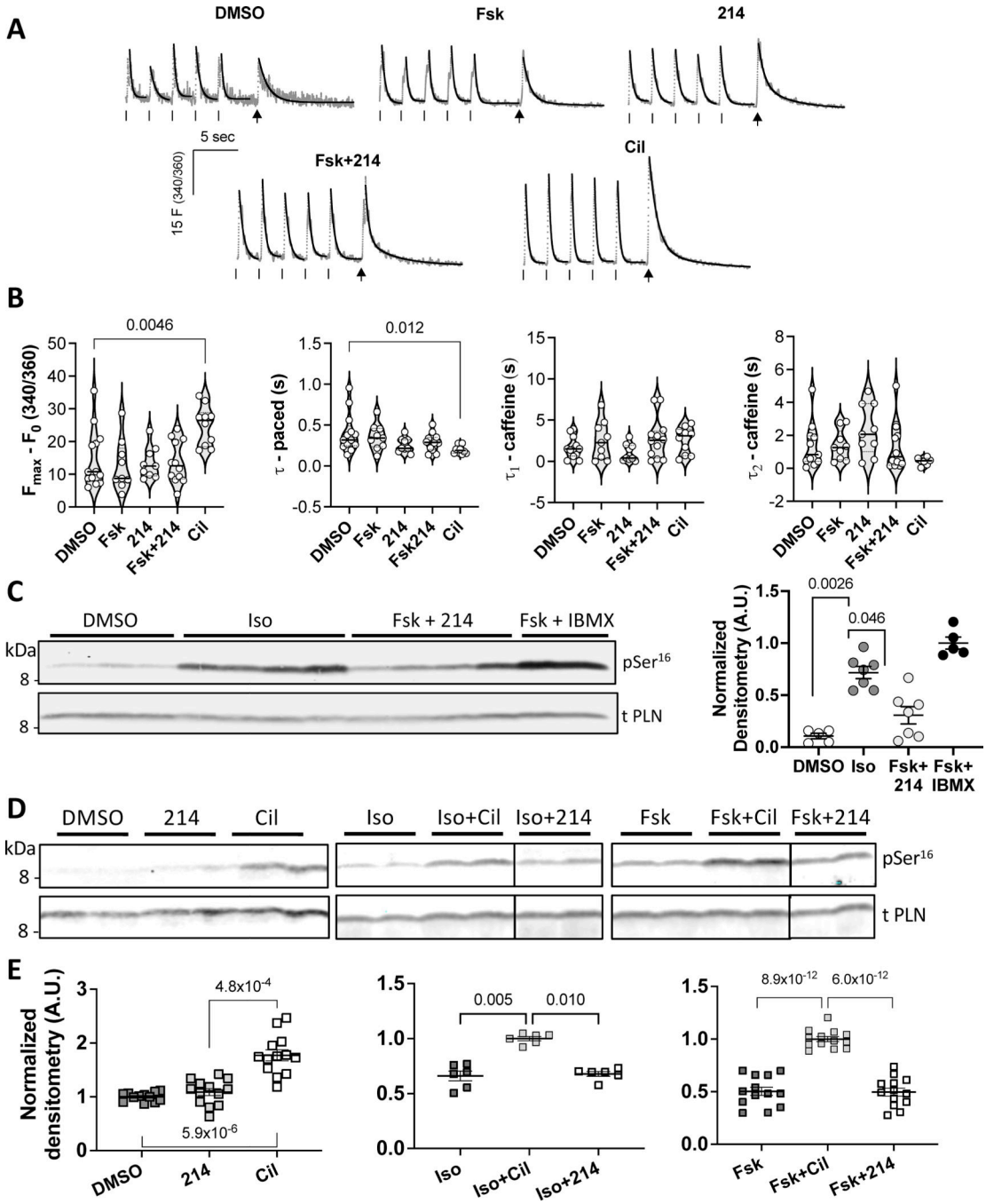

Figure 4. Effects of PDE1i upon SR Ca^{2+} content or phospholamban (PLN) phosphorylation at Ser^{16}.

Guinea pig myocytes treated with: DMSO (vehicle), Fsk (10nM), 214 (1μM), Fsk+214 (1μM), or Cil (1μM), were paced. Then pacing was stopped and cells were exposed to a bolus of caffeine (10mM) to assess SR Ca^{2+} content. **A)** Representative Ca^{2+} traces are shown in grey with exponential decay fits overlaid in black. Ticks indicate pacing; arrows indicate caffeine spritz. **B)** Grouped average changes in the peak Ca^{2+} transients and tau values for systolic and caffeine transients are plotted; Kruskal-Wallis with Dunn's

MCT vs DMSO. **C)** Representative western blot of phosphorylated (Ser^{16}) and total PLN for myocytes treated with Iso at near maximal dose (50nM), Fsk (10nM) + 214 (1μM) or Fsk + IBMX, with quantitation to the right (phospho/total PLN densitometry value normalized to that of Fsk+IBMX; Kruskal-Wallis with Dunn's MCT among DMSO, Iso and Fsk+214). **D)** Western blots and **E)** corresponding quantitation showing change in Ser^{16} phospho/total PLN in response to PDE inhibition at baseline (left; normalized to DMSO) or in combination with: non-saturating dose of Iso (1nM; center; normalized to Iso+Cil) or Fsk (10nM; right; normalized to Fsk+Cil). Kruskal-Wallis with Dunn's MCT vs normalized group for left and center; ordinary 1-way ANOVA with Bonferroni MCT vs normalized group for the right graph.

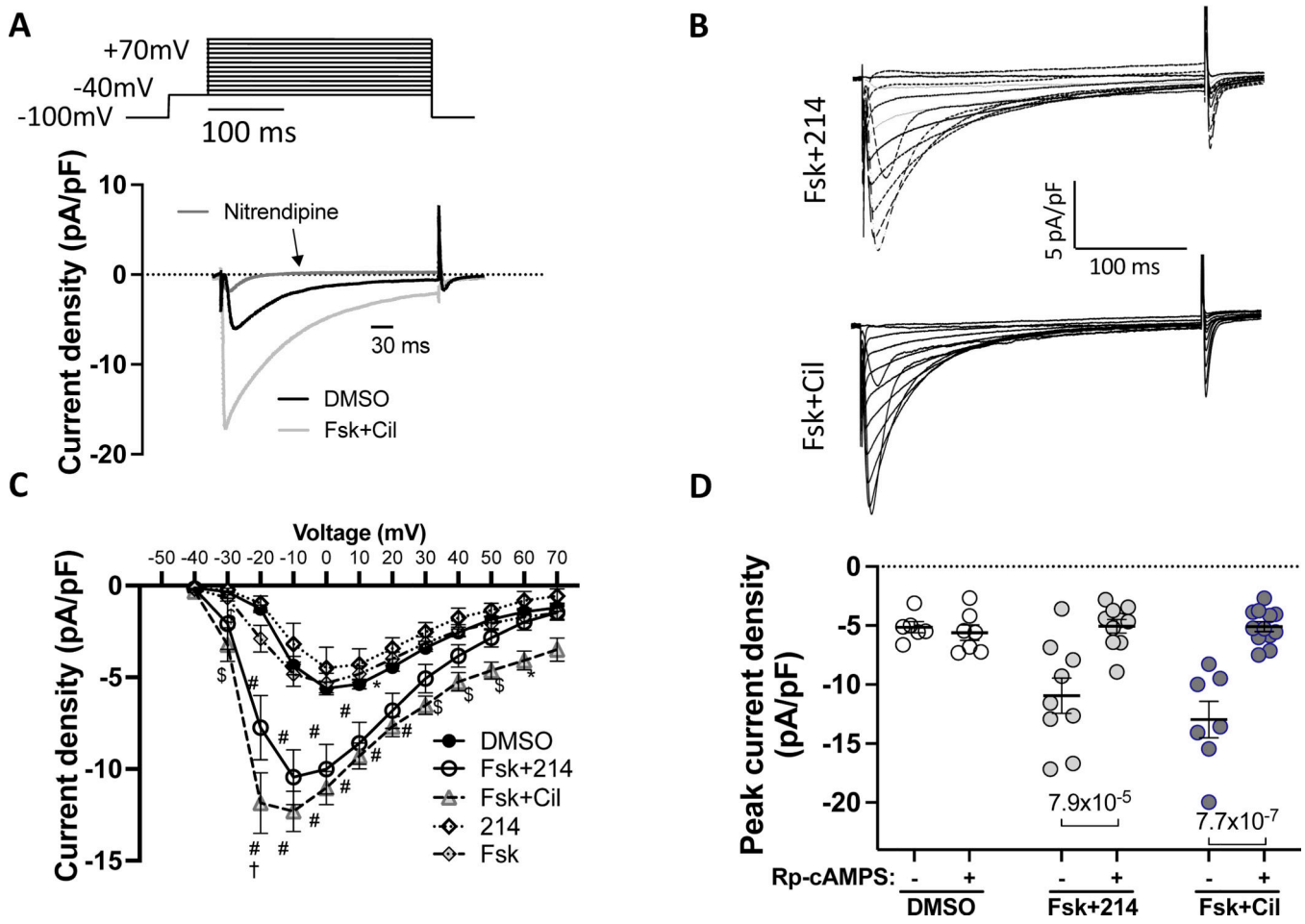

Figure 5. The L-type Ca^{2+} channel $Ca_v1.2$ current increases upon PDE1 or 3 inhibition.

Cells were stimulated with the indicated drugs, and the inward current measured using the whole-cell voltage clamp protocol. Nitrendipine (10μM) was used to confirm $Ca_v1.2$ as the primary source of the current. **A)** The voltage-clamp protocol with representative trace showing change upon Fsk+Cil treatment and sensitivity to nitrendipine. **B)** Representative current-time traces for Fsk+214 and Fsk+Cil. **C)** Averaged peak current density versus membrane voltage. *p<0.05, $p<0.001, #p<0.0001 against DMSO; †p<0.0001 against Fsk+214, ordinary 2-way ANOVA with Tukey's MCT comparing DMSO vs Fsk+214 vs Fsk+Cil; see Online Table I for exact p values. **D)** The peak current density in cells stimulated with indicated drugs before or 8–10 minutes after dialysis with PKA inhibitor - Rp-cAMPS (100μM); ordinary 2-way ANOVA with Sidak's MCT.

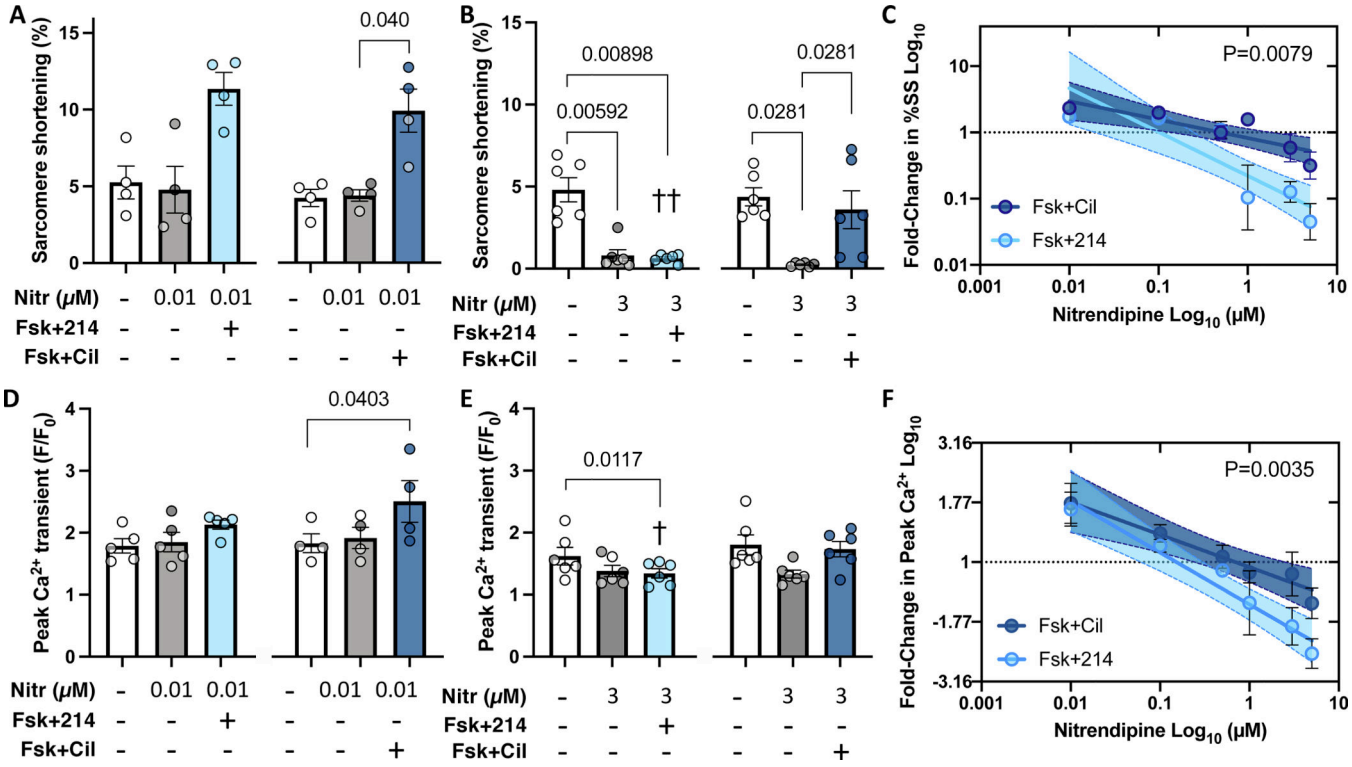

Figure 6. Positive inotropy from PDE1i has greater sensitivity to $Ca_V1.2$ blockade than that from PDE3i.

Myocytes were pre-treated with nitrendipine (Nitr) before further stimulation with Fsk+214 or Fsk+Cil. **A,B)** Sarcomere shortening with Nitr at either 0.01μM or 3 μM. P values in bar graphs from Friedman test with Dunn's MCT within each 3-condition group between all pairs. **C)** Fold-change in sarcomere shortening (%SS) from PDE inhibitor versus DMSO alone plot versus Nitr dose on log-log scale. Linear fit and 95% CI values are shown. P-value for difference in slope of two relations by ANCOVA. **D, E)** Peak Ca^{2+} transient for same treatments shown in panels **A** and **B**, with same statistical test used. ††p=0.0048, †p=0.042 vs respective Nitr+Fsk+Cil group, RM 2-way ANOVA with Holm-Sidak's post-hoc analysis, comparing Nitr ± Fsk+214 or ± Fsk+Cil. **F)** Fold change in peak Ca^{2+} versus Nitr dose for both PDE inhibitors plot and analyzed as in panel **C**. P value is difference in intercept.

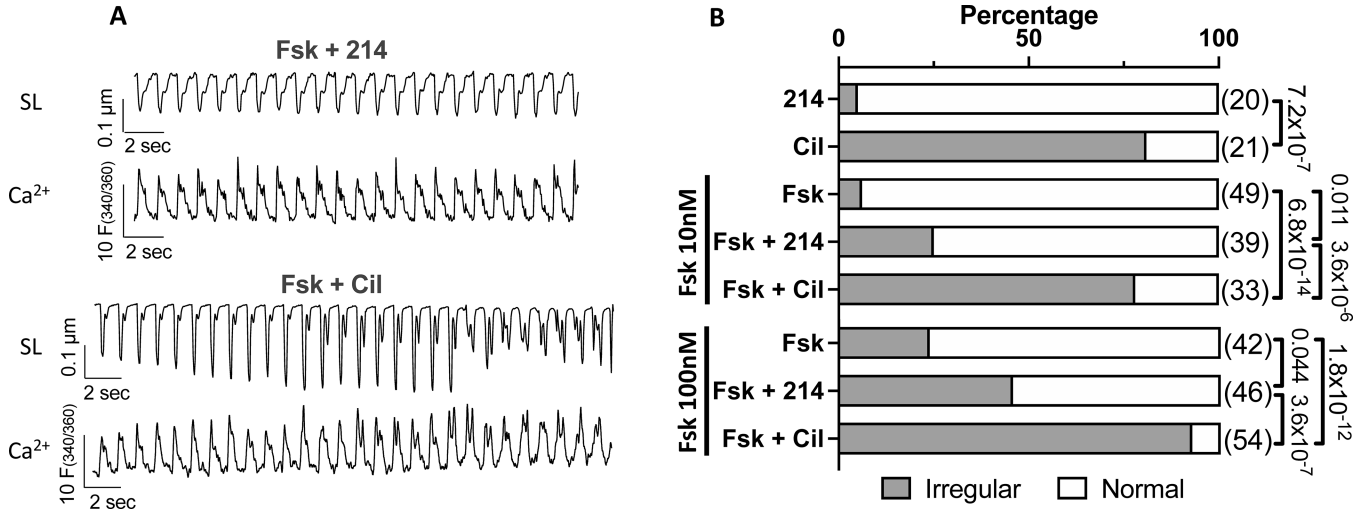

Figure 7. PDE3i stimulates greater irregularity of Ca^{2+} release and contraction over PDE1i.

Myocytes treated with 214 or Cil in the presence of Fsk (0, 10, 100 nM) were scored as normal or irregular. **A)** Representative sarcomere length (SL) and Ca^{2+} transient tracings for cells responding to 214 or Cil in the presence of Fsk (10nM). **B)** The percentage of cells in irregular contractions (grey) or normal (white) for indicated conditions; Fisher's exact test, with n numbers indicated in parenthesis.

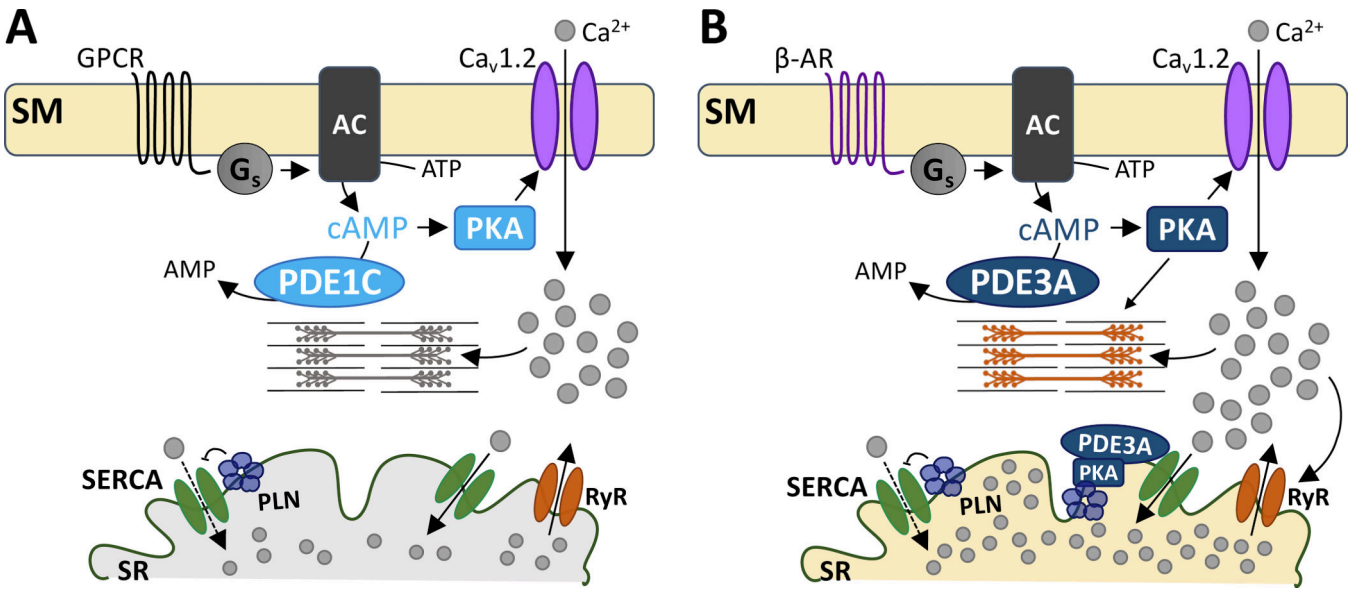

Figure 8. Schematic of the proposed working model.

While both PDEs 1 and 3 hydrolyze cAMP, they do so in distinct microdomains. A) G-protein coupled receptor signals to G_s protein to increase cAMP production. PKA activation subsequently increases $Ca_v1.2$ activity, allowing Ca^{2+} entry and cell shortening. PDE1C is at this domain, hydrolyzing sarcolemmal cAMP. B) PDE3A hydrolyzes both the sarcolemmal and a different pool of cAMP at the SR. At the sarcolemma, PDE3A-hydrolyzes cAMP that is produced by β-AR stimulation. PKA-mediated $Ca_v1.2$ activity leads to increased SR Ca^{2+} reuptake, because of PDE3A's functions at the SR. At the SR, PDE3A controls cAMP/PKA signaling. PKA phosphorylation of PLN releases its inhibition of SERCA-mediated Ca^{2+} reuptake. This augments Ca^{2+}-induced Ca^{2+} release to augment cell shortening. Abbreviations: sarcolemmal membrane (SM), G-protein coupled receptor (GPCR), β-adrenergic receptor (β-AR), stimulatory G protein (G_s), adenylyl cyclase (AC), phosphodiesterase 1C (PDE1C), phosphodiesterase 3A (PDE3A), protein kinase A (PKA), sarcoplasmic reticulum (SR), SR Ca^{2+} ATPase (SERCA), phospholamban (PLN), ryanodine receptor (RyR).

Table 1.

Myofilament parameters in skinned guinea pig myocytes

	DMSO	Iso	Fsk+214
Fmax	20 ± 1.9	23 ± 3.6	16 ± 2.4
EC_{50}	2.4 ± 0.12	4.6 ± 0.69	2.8 ± 0.57
Hill's coefficient	5.5 ± 1	3.3 ± 0.58	3.9 ± 0.69